AFF-1 fusogen can rejuvenate the regenerative potential of adult dendritic trees via self-fusion

Veronika Kravtsov[1,#], Meital Oren-Suissa[1,#], and Benjamin Podbilewicz[1†]

[1]Department of Biology, Technion- Israel Institute of Technology, Haifa 32000, Israel

[#]These authors contributed equally to this work

[†]Correspondence to: podbilew@technion.ac.il

Running title: Neuronal anti-aging by fusion

Key words: AFF-1, dendritic remodeling, *Caenorhabditis elegans*, regeneration by self-fusion

Summary statement: Ectopic expression of AFF-1 fusogen or low activity of IGF-1R/DAF-2 rejuvenate the regeneration potential of dendrites following injury in aging *C. elegans*

Abstract

The aging brain undergoes structural changes, affecting brain homeostasis, neuronal function and consequently cognition. The complex architecture of dendritic arbors poses a challenge to understanding age-dependent morphological alterations, behavioral plasticity and remodeling following brain injury. Here, we use the PVD polymodal neurons of *C. elegans* as a model to study how aging affects neuronal plasticity. Using confocal live imaging of *C. elegans* PVD neurons, we demonstrate age-related progressive morphological alterations of intricate dendritic arbors. We show that insulin/IGF-1 receptor mutations (*daf-2*) fail to inhibit the progressive morphological aging of dendrites and do not prevent the minor decline in response to harsh touch during aging. We uncovered that PVD aging is characterized by a major decline in regenerative potential of dendrites following experimental laser dendrotomy. Furthermore, the remodeling of transected dendritic trees via AFF-1-mediated self-fusion can be restored in old animals by DAF-2 insulin/IGF-1 receptor mutations, and can be differentially reestablished by ectopic expression of AFF-1 fusion protein (fusogen). Thus, AFF-1 fusogen ectopically expressed in the PVD and mutations in DAF-2/IGF-1R, differentially rejuvenate some aspects of dendritic regeneration following injury.

35 **Introduction**

36 Aging is the primary risk for neuronal diseases and general cognitive decline in humans
37 (Yankner et al., 2008), yet, our understanding of the process of neuronal aging at the
38 molecular and cell biological levels is still limited. In particular, very few studies have
39 investigated the fate of complex dendritic arbors during aging, and their regenerative capacity
40 following brain injury or trauma. Signaling via the DAF-2 Insulin/IGF-1 receptor is the most
41 prominent and conserved pathway that controls aging and longevity of *C. elegans*, flies, and
42 mammals (Kenyon, 2010). *C. elegans* is a powerful system to study the genetics of neuronal
43 aging and regeneration (Ghosh-Roy and Chisholm, 2010; Hammarlund and Jin, 2014;
44 Kenyon, 2010). Normally, when the DAF-2/IGF-1 receptor is activated it induces a
45 conserved PI3K/AKT kinase cascade, which in turn inhibits the DAF-16/FOXO transcription
46 factor from entering into the nucleus. Reduction of *daf-2* function doubles life span, and
47 long-lived worms are considered to stay healthy for longer (Kenyon et al., 1993; Kenyon,
48 2010). In these animals, DAF-16/FOXO affects transcription of different genes that encode
49 heat-shock proteins, antimicrobial proteins, antioxidants, and other molecules, which leads
50 ultimately to extended lifespan (Lin et al., 2001; Murphy et al., 2003). Recently, aging-
51 associated axonal morphological alterations and decline in regenerative capacity were
52 described in *C. elegans*. *daf-2* mutations delayed these age-related morphological changes
53 and improved regeneration of aged severed axons in a *daf-16*-dependent manner (Byrne et
54 al., 2014; Pan et al., 2011; Tank et al., 2011; Toth et al., 2012). Moreover, in the case of
55 GABA motor neurons, as adult animals age there is a reduction in axon growth, retraction
56 and regrowth in response to injury. Surprisingly, the decline in regeneration by regrowth is
57 controlled by *daf-16* in a cell-autonomously fashion and independently of lifespan (Byrne et
58 al., 2014).

59 The process of regeneration of injured axons in vertebrates and invertebrates often
60 involves degeneration of the distal part followed by regrowth (Chisholm et al., 2016; Park et
61 al., 2008; Ruschel et al., 2015; Taylor et al., 2005; Yaniv et al., 2012). However, different
62 invertebrates, including nematodes and crustaceans, use plasma membrane fusion as an
63 alternative mechanism for repair of injured axons (Ghosh-Roy et al., 2010; Hoy et al., 1967;
64 Neumann et al., 2015; Neumann et al., 2011). Cell fusion events were also observed in the
65 brains of mammals both spontaneously and as a result of injury such as stroke (Alvarez-
66 Dolado et al., 2003; Johansson et al., 2008; Paltsyn et al., 2013), but the role of these events
67 has remained unclear (Giordano-Santini et al., 2016). In *C. elegans*, axonal regeneration via
68 auto-fusion is mediated by the fusogen EFF-1 (Ghosh-Roy et al., 2010; Neumann et al.,
69 2015; Neumann et al., 2011). EFF-1 is the first *bona fide* eukaryotic developmental cell-cell
70 fusion protein. It is expressed in different cell types including neurons, and mediates fusion
71 between cells by a homotypic mechanism (Gattegno et al., 2007; Mohler et al., 2002;
72 Podbilewicz et al., 2006; Shemer et al., 2004). Thus, EFF-1 has to be expressed in both
73 cellular membranes for them to merge and the high-resolution crystal structure of EFF-1
74 ectodomain suggests that EFF-1 acts by a mechanism that is distinct from viral-induced
75 fusion. EFF-1, not only has to be present in both membranes for them to fuse, it also appears
76 to interact in trans forming complexes that tether and fuse the membranes (Pérez-Vargas et
77 al., 2014; Podbilewicz et al., 2006). During embryonic development EFF-1 is kept inactive
78 inside early endosomes via Dynamin- and RAB-5-mediated endocytosis (Smurova and
79 Podbilewicz, 2016).
80 We have been studying the role of fusion proteins in the PVD neuron, a polymodal
81 nociceptor that senses harsh touch to the body, cold temperature, and posture (Chatzigeorgiou
82 et al., 2010; Oren-Suissa et al., 2010; Smith et al., 2010; Tsalik et al., 2003). The PVD
83 neuron exhibits an elaborate and invariant dendritic structure, which is composed of a

84 repetitive unit that resembles a candelabrum (or a "menorah") **(Fig 1A)** (Oren-Suissa et al.,
85 2010). These dendritic trees arise and are dynamically maintained through several intrinsic
86 and extrinsic genetic pathways (Chatzigeorgiou et al., 2010; Cohen et al., 2014; Dong et al.,
87 2013; Dong et al., 2015; Husson et al., 2012; Liu and Shen, 2011; Maniar et al., 2012; Oren-
88 Suissa et al., 2010; Salzberg et al., 2013; Smith et al., 2010; Wei et al., 2015).
89 The PVD develops in a stereotypic fashion from the L2 larval stage to the young adult
90 (Oren-Suissa et al., 2010). The fusion protein EFF-1 mediates dendrite retraction and auto-
91 fusion of excess branches by a novel cell-autonomous pruning mechanism (Oren-Suissa et
92 al., 2010). Thus, this fusogen maintains the structural units by trimming excess branching
93 during normal developmental arborization (Oren-Suissa et al., 2010). AFF-1, a paralog of
94 EFF-1, is a second *C. elegans* fusogen displaying a more restricted tissue distribution pattern
95 (Avinoam and Podbilewicz, 2011; Sapir et al., 2007); AFF-1 was not found to be involved in
96 PVD remodeling during development (Oren-Suissa et al., 2017). AFF-1 and EFF-1 fusion
97 proteins also auto-fuse epithelial and myoepithelial cells to form tubes and reshape glial cells
98 (Procko et al., 2011; Rasmussen et al., 2008; Soulavie and Sundaram, 2016; Stone et al.,
99 2009). Moreover, it has recently been demonstrated that in vertebrates auto-fusion takes
100 place in the development of the vascular endothelium, where it leads to pruning of excess
101 blood vessels (Lenard et al., 2015) in a process that remarkably resembles EFF-1-mediated
102 PVD pruning (Oren-Suissa et al., 2010) and that may link EFF-1 to the actin cytoskeleton.
103 Recently it was reported that during larval development, EFF-1 interacts with filamentous
104 actin via Spectraplakin (VAB-10A) to maintain EFF-1 at the site of epidermal cell fusion
105 (Yang et al., 2017). The pathway of PVD dendritic repair following laser-induced
106 dendrotomy and the functions of EFF-1 and AFF-1 were recently established (Oren-Suissa et
107 al., 2017). The mechanism of PVD dendritic regeneration following injury can be divided in
108 five overlapping stages: (1) reattachment at site of injury, (2) loss of self-avoidance between

109 adjacent menorahs, (3) AFF-1-dependent menorah-menorah fusion that can bypass the
110 lesions, (4) sprouting of compensatory dendrites and (5) EFF-1-dependent trimming of
111 excess branches. It is unknown whether PVD structure and function is affected by aging and
112 by the activity of fusion proteins.

113 Here, we show that induction of cellular fusion proteins (fusogens) can remodel and
114 facilitate regeneration of dendrites in polymodal PVD neurons of aging *Caenorhabditis*
115 *elegans*. Using whole-animal live imaging, we find that the PVD dendritic trees, composed of
116 repetitive orderly multibranched units, show age-dependent hyperbranching, disorganization,
117 and loss of self-avoidance. These processes, while independent of canonical lifespan-
118 regulating pathways, can be partially rescued by ectopic expression of the fusogen EFF-1 that
119 prunes multibranched dendrites. Surprisingly, most wild-type and *daf-2* (Insulin/IGF-
120 1Receptor) mutant adults that have disorganized dendritic trees have normal response to
121 harsh touch. Furthermore, we found a decreased capacity of old animals to repair laser-
122 induced injured dendrites via auto-fusion that can be restored by reducing DAF-2 function or
123 by ectopic expression of the EFF-1 paralog AFF-1 that remodels dendritic trees via merging
124 of injured branches. Our findings demonstrate that fusogens are sufficient to maintain the
125 dendritic arbor structure and increase its regeneration potential by auto-fusion in aging
126 animals. These anti-aging strategies can be potentially applied to other organisms to help
127 them recover from stroke, brain trauma and spinal cord injury.
128

129 **Results**

130 **Progressive dendritic remodeling during aging is independent from the Insulin/IGF-1**
131 **pathway**

132 Aging neurons lose their ability to remodel following injury, change their complex
133 morphology, and may degenerate (Yankner et al., 2008). Whereas axon degeneration during

134 aging has been studied extensively both in mammals and in invertebrates, the fate of complex
135 dendritic trees in old animals has not been studied in detail in any organism. To determine
136 how aging affects the complex arborized dendritic structure, we analyzed the *C. elegans* PVD
137 dendritic branching patterns from the fourth larval stage (L4) to ten-day-old adults. We found
138 that during aging PVD's dendritic structures undergo disorganization and hyperbranching
139 **(Figs 1A, 1C, and S1)**. Remarkably, we found that these age-dependent morphological
140 changes of the PVD dendritic pattern were not affected in long-lived animals carrying a
141 mutation in *daf-2* **(Figs 1A-1H, and S1)**. Adjacent PVD dendrites normally avoid each other
142 (Smith et al., 2012), and we found that as the animal ages the structural units lose their self-
143 avoidance properties **(Fig 1C, 1D, and 1I)**. Consistently, this age-dependent dendritic
144 pattern did not improve in *daf-2* mutant animals; young *daf-2* animals at the L4 stage
145 exhibited significantly more *daf-16*-dependent self-avoidance deficiencies in comparison to
146 wild-type **(Fig 2)**. Thus, taken together our results reveal that during aging there is a *daf-2*-
147 independent increase in disorganization of branching and loss of self-avoidance.
148 The elaborate PVD structure is highly dynamic in young animals, exhibiting constant
149 growth and retraction of individual high order branches (Oren-Suissa et al., 2010; Smith et
150 al., 2010; Smith et al., 2012). To further understand the dynamics of the age-dependent
151 dendritic tree remodeling, we followed individual animals over time and analyzed time-lapse
152 movies. We found that 5-day adults still exhibited some plasticity of the dendritic tree, with
153 dynamic growth and retraction events **(Fig 3A** and **Movie S1)**; however, both growth and
154 retraction were two times slower **(Fig 3B)** compared to younger L4 animals, imaged under
155 the same conditions. Next we quantified the number of movements of branches. Most
156 branches showed dynamic movements ending either with elongation or with shortening, but a
157 minority of branches only grew or only retracted throughout the movies. When young
158 animals were imaged, not only the rates of growth and retraction were higher, but also the

159 number of dynamic events involving both growth and retraction were higher (data not
160 shown). Interestingly, both in L4 larvae and 5d adults there were more events that ended with
161 outgrowth or elongation rather than retraction events. We also found that the decrease in
162 dynamic events with age was proportional both for outgrowth and retraction **(Fig 3B).** Thus,
163 we conclude that at all ages there are slightly more growth events than retractions, which
164 leads to branch accumulation with time and thus causing hyperbranched phenotype of the
165 PVD. These experiments reveal that the PVD dendritic arbors grow and age in a dynamic
166 way and not in a step-wise manner as apparent from still images. This dynamic growth and
167 retraction together with the increase in branching as animals age suggest that hyperbranching
168 is part of the normal dynamic growth of the dendritic arbors.

169 We speculated that reduced dendritic plasticity and structural changes in aged animals
170 would affect the functionality of the PVD neurons. To shed more light on the link between
171 structure and function of dendrites during aging, we performed a functionality test. PVD
172 responds to harsh stimulations, and we used a classic harsh touch assay in *mec-4* mutant
173 animals to specifically test PVD activity without the background light touch response
174 mediated by the six light-touch mechanosensory neurons (Oren-Suissa et al., 2010; Way and
175 Chalfie, 1989). First, we found that although *mec-4* animals have shorter life span (Pan et al.,
176 2011), their dendrites looked similar to wild-type between the ages L4-5d **(Fig 4)**, which
177 further demonstrates that the morphological alterations we see are lifespan-independent.
178 Second, we found that the PVD functionality showed a minor decrease with aging, with 5d
179 adults presenting a small but significantly reduced harsh touch response in comparison to 1d
180 adults, in both *mec-4* and *mec-4;daf-2* double mutants **(Fig 4F)**. Harsh touch to the body was
181 measured by prodding animals with a platinum wire in the midsection of the body (Oren-
182 Suissa et al., 2010; Way and Chalfie, 1989). We cannot rule out that multiple components of
183 the sensorimotor circuit contribute to the age-dependent decline in PVD activities. Thus, our

184 results reveal that the morphological and behavioral hallmarks of aging in PVD dendritic
185 arbors are independent from the canonical IGF-1 pathway that affects lifespan. Moreover, the
186 fact that the dramatic increase in branching and loss of self-avoidance in middle-aged animals
187 (5d-adults; **Figs 1-3**) correlates with lack of response to harsh touch in only 10% of the
188 worms, compared to 1d adults, suggests that hyperbranching, loss of self avoidance and
189 disorganization of dendritic trees might be normal and not deleterious for the behavioral
190 response.

191 In summary, the changes in dendritic architecture are not necessarily a deleterious
192 aspect of aging, but could actually be part of normal neuronal maintenance that keeps the cell
193 functioning over time. The fact that they are not altered in *daf-2* mutants supports this idea, as
194 does the functional data that shows most of the neurons function fine in 5 days adults (**Fig 4**).
195 Thus, the observed increase in dendrite branching and the disorganized appearance of the
196 trees is probably adaptive as the animals increase in girth.

197 **Age-dependent dendrites remodeling can be modulated by EFF-1**

198 The fusogen EFF-1 is essential to fuse some injured axons in *C. elegans* (Ghosh-Roy et al.,
199 2010; Neumann et al., 2015), and is involved in PVD's dendrite pruning in a cell-autonomous
200 and dosage-dependent manner during development and in young adults (Oren-Suissa et al.,
201 2010). When EFF-1 is overexpressed in the PVD, a strong gradient of arborization is seen in
202 L4s and young adults, with almost complete lack of branches in areas that are distal from the
203 cell body. However, in areas around the cell body the PVD menorahs appear similar to those
204 in the wild-type (Oren-Suissa et al., 2010) **(Fig 5A** and **5B)**. Since EFF-1 retracts and
205 simplifies dendritic arbors in young animals (Oren-Suissa et al., 2010) and is expressed in the
206 PVD throughout adulthood (**Fig S2**), we hypothesized that EFF-1 overexpression will be able
207 to retract dendrites in aged adults. Indeed we found that EFF-1 overexpression in the PVDs
208 simplified the hyperbranching around the cell body at 9-10 days adults **(Fig 5C-5E)**; in

209 particular, the quaternary branch order was decreased **(Fig 5F)**. A trend of reduction in fifth
210 and higher order branches also appeared in aged animals overexpressing EFF-1 **(Fig 5G)**.
211 Thus, overexpression of the fusogen EFF-1 in the PVD neuron is sufficient to simplify aged
212 menorahs. These results suggest that there is a reduction in EFF-1 expression in old animals,
213 or a decreased efficiency of EFF-1 activity in older animals. We quantified the expression
214 levels of EFF-1 in the PVD throughout development and found a reduction in the number of
215 EFF-1 puncta in aged animals **(Fig. S3)**. In contrast to *eff-1*, *aff-1* mutants have no evident
216 morphological phenotypes in the PVD and its expression has not been detected in this neuron
217 (**Fig S2;** (Oren-Suissa et al., 2017)); moreover, when AFF-1 is ectopically expressed in the
218 PVD in an *eff-1* mutant background it does not retract excess branching, demonstrating that it
219 is unable to rescue the pruning defects of *eff-1* **(Fig S4)**. This result shows that EFF-1 and
220 AFF-1 fusion proteins have different activities and are not interchangeable in the PVD
221 neuron. In summary, during normal aging there is a reduction of EFF-1 expression that
222 appears to result in an increase in dendritic branching. We can reverse the hyperbranching
223 age-related phenotype by ectopic expression of EFF-1 in older animals, which simplifies the
224 morphology of PVD dendritic arbors.

225 **Age-dependent decline in dendrite regeneration is dependent on Insulin/IGF-1**

226 Mammalian axons regenerate better in younger individuals than in adults (Verdu et al.,
227 2000). Similarly, axonal regenerative ability declines drastically as nematodes advance
228 through development and age (Byrne et al., 2014; Zou et al., 2013). Our knowledge is still
229 poor on the regenerative capacity of the dendrite, and how aging affects this process of
230 neuronal repair (Bekkers and Hausser, 2007; Nawabi et al., 2012; Rao et al., 2016). To study
231 dendritic regeneration we severed the primary dendrites of PVD neuron in aging adults.
232 Typically, the PVDs show robust regeneration at L4 larval stage, consisting in dendrite
233 sprouting from the proximal fragment still attached to the cell body and reconnection via

234 fusion with the separated distal dendrite fragment **(Fig 6A, Movie S2**; (Oren-Suissa et al.,
235 2017)). To directly measure reconnection by auto-fusion, we used the photoconvertible
236 reporter Kaede **(Fig S5 and Movie S3)**. If fusion fails to occur, the detached distal part
237 eventually degenerates. We found that 2-3 day-old wild-type adults respond more slowly to
238 laser dendrotomy in comparison to L4 and young adults (~70% of the young animals
239 presented regeneration, whereas at the age of 2-3d neither regeneration nor degeneration
240 occurred within 3-6 hours (**Fig 6E and Movie S4)**. At the age of 5 days, the ability to
241 regenerate by dendrite auto-fusion was almost completely lost **(Fig 6C** and **6F)**. Thus, we
242 found that relatively young adults already show a decline in their dendritic regenerative
243 ability.

244 To determine whether the decline in the ability to remodel dendrites by auto-fusion is
245 dependent on the Insulin/IGF-1 pathway we tested whether the long-lived *daf-2* mutants are
246 prevented from losing their dendritic self-fusion ability. We found that *daf-2* mutants showed
247 similar regeneration to wild-type at L4 stage **(Fig 6B** and **6F)**, whereas at older age (5d) *daf-2*
248 mutants had a much higher regenerative ability than wild-types (70% successful regeneration
249 in *daf-2* versus 12.5% in wild-type) **(Fig 6D** and **6F)**. Similarly to axonal response to injury
250 (Byrne et al., 2014), we found that DAF-2 inhibits regeneration of aged dendrites through
251 inhibition of DAF-16, as *daf-16* mutants and *daf-2;daf-16* double mutants showed
252 regenerative decline during aging similar to wild-type **(Fig 6F)**. In conclusion, our results
253 reveal that dendrite regeneration following transection declines with aging, a phenotype that
254 is dependent on DAF-2/IGF-1R and its target DAF-16/FOXO.

255 **AFF-1 mediates and restores dendrite regeneration in aged animals**

256 AFF-1 (Anchor cell Fusion Failure 1), is a transmembrane protein related to EFF-1 that
257 executes several cell-cell fusion events during development in the epidermis, excretory,
258 digestive and reproductive systems (Sapir et al., 2007). We have recently dissected the

259 cellular pathway for dendritic remodeling following PVD injury (Oren-Suissa et al., 2017).
260 We showed that injured primary dendrites regenerate and reattach at the site of injury via
261 self-cell fusion. Simultaneously, terminal branches lose self-avoidance and grow towards
262 each other, meeting and fusing via an AFF-1-mediated process. Throughout the regeneration
263 process sprouting of compensatory branches occurs, and simplification of the dendritic arbors
264 completes the regeneration process through *eff-1*-dependent pruning and retraction of excess
265 branches. We found that AFF-1 functions cell non-autonomously from the epidermal seam
266 cells and we hypothesize that AFF-1-containing extracellular vesicles fuse injured neuronal
267 dendrites from without (Oren-Suissa et al., 2017).

268 Adults carrying loss-of-function mutations in *aff-1* have severe egg laying defects,
269 shorter life spans and excretory system defects that prevented us from studying regeneration
270 in aging *aff-1* mutant animals. To investigate whether AFF-1 can autonomously restore the
271 regenerative ability of dendrites in older animals we overexpressed AFF-1 specifically in the
272 PVD (PVDp::AFF-1; **Fig S6**). We found that the structural units of young animals expressing
273 PVDp::AFF-1 appeared morphologically wild-type and responded similarly to dendrotomy
274 **(Fig 7A, Movie S5)**. However, when 5-day old PVDp::AFF-1 animals were dendrotomized,
275 the percentage of regenerating worms by dendrite fusion was significantly higher compared
276 to wild-type animals (60-80% and 13%, respectively; **Fig 7B and 7C, Movie S6)**. Thus,
277 AFF-1-specific overexpression in the PVD enables dendrite regeneration via auto-fusion of
278 cut dendrites in older animals **(Fig 7C)**.

279 To determine whether *daf-2*(-) or PVDp::AFF-1 affect PVD architecture following
280 injury independently of the remodeling by self-fusion, we quantified the number of PVD
281 branches before and after injury in L4 and 5d adults. We found that only L4 animals
282 expressing PVDp::AFF-1 showed an increase in the number of branches 24 hours post injury
283 (Fig S7). Old 5d animals expressing PVDp::AFF-1 did not exhibit any difference in the

284 number of branches as compared with wild-type and *daf-2* mutant animals, before and after
285 injury. We also tested whether animals overexpressing AFF-1 have functional PVDs
286 comparable to wild-type animals, by testing the behavioral response of PVDp::AFF-1
287 animals to harsh touch. We found that 80% PVDp::AFF-1 responding 5d adult animals
288 (n=59), compared to control animals with 88% responding (n=75). These results suggest that
289 there is no correlation between the ability to respond to harsh touch and the number of
290 branches as a consequence of the expression of AFF-1 in the PVD. The main factor
291 maintaining PVD activity is whether it regenerates via AFF-1-mediated auto-fusion
292 following an injury, because it regenerates the complete dendritic tree structure. Taken
293 together, the autonomous and ectopic expression of the fusion protein AFF-1 in the PVD
294 appears to rejuvenate the ability to reconnect cut dendrites by the self-fusion mechanism.
295 Since endogenous AFF-1 expression cannot be detected in the PVD ((Oren-Suissa et al.,
296 2017); Fig. S2), it appears that ectopic activity of the AFF-1 fusion protein in the PVD
297 neuron is sufficient to repair and remodel severed dendrites via the mechanism of auto-fusion
298 in middle aged adults.

299 **Rejuvenation of fusion potential of cut dendrites by *daf-2(-)* and AFF-1(+)**

300 We wished to further compare the regenerative modalities of AFF-1 overexpression and *daf-*
301 *2* mutation following dendritic laser-induced severing in aging animals. Dendritic fusion
302 following injury can occur by three possible pathways: 1) 3ry-3ry branch fusions that bypass
303 the injury site ("menorah-menorah" fusion); 2) fusion of the proximal primary (1ry) branch to
304 the detached distal 1ry; 3) both 3ry-3ry fusion and 1ry-1ry fusion **(Fig 8A)**. To determine
305 whether the mechanism of remodeling of dendritic trees following injury is distinct in wild-
306 type, *daf-2* reduced function mutants and in animals ectopically expressing AFF-1 in the
307 PVD, we compared the remodeling of dendritic trees in aging animals in these three
308 genotypes following injury. We found that in wild-type and PVDp::AFF-1 animals at the L4

309 stage, the most prevalent mechanism of repair is 3ry-3ry fusion (pathway 1), whereas in *daf-2*
310 mutants 3ry-3ry fusion together with 1ry-1ry fusion (pathway 3) increased compared to wild-
311 type **(Fig 8B-8D)**. In wild-type, we found degeneration in 50% (2-4d) and 80% (5-6d) of the
312 dendrotomized animals **(Fig 8E** and **8H)**. Adult *daf-2* mutant animals (5-6d) presented a
313 response to injury that resembled that observed in L4 wild-type animals, with 70% of the
314 animals showing regeneration, mainly via 3ry-3ry fusions **(Fig 8F** and **8I)**. In contrast, in
315 PVDp::AFF-1 animals the response to injury followed a different mechanism, with more
316 regeneration via enhanced 1ry-1ry fusion instead of 3ry-3ry fusion as observed in *daf-2*
317 mutants **(Fig 8G** and **8J).** However, the AFF-1 effect was unrelated to longevity as
318 PVDp::AFF-1 animals had normal lifespans **(Fig S8)**. Thus, differential activities of AFF-
319 1(+) and *daf-2*(-) maintain the remodeling potential of aging arbors, and the mechanisms of
320 rejuvenation by fusion that prevent degeneration appear to be independent. In both cases
321 degeneration of the distal trees is prevented.
322 Aged dendritic trees lose their regenerative potential because following laser-induced
323 dendrotomy old neurons usually fail to auto-fuse broken dendrites and undergo degeneration.
324 DAF-2/ IGF-1R negatively regulates the regeneration process. When the fusogen AFF-1 is
325 ectopically expressed in the PVD neuron it has an antiaging activity that promotes auto-
326 fusion of old transected primary dendrites.
327
328 **Discussion**
329 Precise dendritic arborization is critical for proper functioning of neuronal networks, while
330 defective dendritic development and maintenance lead to neuropathologies (Jan and Jan,
331 2010; Koleske, 2013). There is evidence from mammalian CNS showing increase in number
332 and length of terminal dendritic arbors during aging, and reduced arborization in senile
333 dementia (Buell and Coleman, 1979). However, it remains unclear whether there is a direct

334 link between altered dendritic structure and reduced function in mammals and other
335 organisms (Maletic-Savatic et al., 1999; Thompson-Peer et al., 2016). Axons of aging
336 neurons also show altered morphologies in diverse species. In *C. elegans* these axonal
337 alterations are not affected by organismal longevity (Byrne et al., 2014; Hammarlund et al.,
338 2009; Verdu et al., 2000; Zou et al., 2013). Here we also found that dendritic alterations
339 during aging are not affected by chronological age; however, unlike the PVD dendrites, in
340 axons the *daf-2* mutation was found to delay the morphological alterations of aged animals
341 (Pan et al., 2011; Tank et al., 2011; Toth et al., 2012). Nevertheless, the *daf-2* effect in age-
342 related axonal branching was reported to be uncoupled of its role in extending the lifespan of
343 the worms (Tank et al., 2011; Toth et al., 2012). It thus appears that DAF-2 is specifically
344 involved in cell-autonomous pathways that maintain axonal, but not dendritic morphology.
345 We observed a small but significant decline in response to harsh touch during aging in both
346 wild-type and *daf-2* **(Fig. 4).** Thus, we propose that the dendrite overgrowth observed in old
347 animals reveal a reduction in morphological plasticity and a normal change in the architecture
348 of the dendritic trees that do not appear to have major functional consequences in the ability
349 to respond to noxious mechanosensory stimuli. However, the link between structure and
350 function needs to be further investigated in future studies. While progressive age-related
351 hyperbranching of the PVD arbors was independent of insulin/IGF-1 pathway,
352 overexpression of EFF-1 in the PVD was sufficient to partially rescue this phenotype in old
353 animals (**Figs 5 and 9**). EFF-1 appears to act cell-autonomously to simplify the dendritic
354 trees via its pruning activity mediated by branch retraction (Oren-Suissa et al., 2010).
355 We further found that dendrite regeneration following PVD dendrotomy decreases
356 with age. This decline was "rescued" in *daf-2* mutants (**Fig 6**). Thus, repair of injured
357 dendrites is *daf-2*-dependent whereas the hyperbranching is not (**Figs 1, 6 and 9**). Axonal
358 regeneration is known to decline with age in different organisms (Byrne et al., 2014; Gabel et

359 al., 2008; Hammarlund et al., 2009; Pestronk et al., 1980; Verdu et al., 2000; Zou et al.,
360 2013). In GABA neurons of *C. elegans* the decline in axonal regeneration is also delayed in
361 *daf-2* mutants (Byrne et al., 2014). However, these neurons do not engage in self-fusion
362 during regeneration, whereas in PVD dendrites the main outcome of regeneration is auto-
363 fusion. Recently, an important role of auto-fusion during axonal regeneration was
364 demonstrated in the PLM sensory neurons of *C. elegans*, a process mediated by the fusogen
365 EFF-1 (Ghosh-Roy et al., 2010; Neumann et al., 2015). In the PVD EFF-1 is not necessary
366 for dendrite reconnection following injury (Oren-Suissa et al., 2017). In the PVD dendrites,
367 this role is fulfilled by the EFF-1 paralog AFF-1. Significantly, when AFF-1 is ectopically
368 expressed, this fusogen plays a role in maintenance of regenerative potential during aging
369 (**Figs 7-9)**. These findings highlight fusion mechanisms as potential target for
370 pharmacological intervention in neuropathologies that result from both injury and aging.
371

372 **Materials and Methods**

373 **Nematode strains**

374 Animals were maintained at 20°C, unless otherwise stated, according to standard protocols
375 (Brenner, 1974). All experiments were performed on hermaphrodites. N2 served as wild-
376 type, and the following mutants and transgenic strains were used:
377 NC1841 *[wdIs52(F49H12.4::GFP); rwIs1(pmec-7::RFP)]* (Smith et al., 2010), outcrossed
378 4X, CHB392 *[hmnEx133(ser-2prom3::kaede)],* kindly provided by Candice Yip and Max
379 Heiman (Yip and Heiman, 2016), BP709 *[hmnIs133 (ser-2prom3::kaede)]*, kindly provided
380 by Tamar Gattegno, MF190 *[hmIs4(des-2::gfp, pRF4)]* (Oren-Suissa et al., 2010). CB1338
381 *[mec-3(e1318)IV]*, *Caenorhabditis* Genetics Center (CGC), CB1611 *[mec-4(e1611)X],*
382 (CGC), BP176 *[hyEx23(des-2::eff-1, des-2::gfp, pRF4)]* (Oren-Suissa et al., 2010), BP177
383 *[hyEx392(des-2::eff-1, des-2::gfp, pRF4)],* BP488 *[eff-1(hy21)II; hmIs4; hyEx39(des-*

384 *2p::AFF-1,myo-2::GFP,KS)]*, BP906 *[daf-2(e1370)III; wdIs52; rwIs1],* BP911 *[hyEx39;*
385 *hmnEx133]*, BP915 *[hyEx39; hmnIs133]*, BP550 *[hyEx391(des-2p::AFF-1, myo-2::GFP,*
386 *KS); hmnEx133],* BP919 *[daf-2(e1370)III; daf-16(mu86)I; hmnIs133],* BP923 *[daf-*
387 *16(mu86)I; hmnIs133]*, BP924 *[daf-2(e1370)III; hmnIs133]*, BP925 *[mec-4(e1611)X;*
388 *hmnIs133],* BP926 *[daf-2(e1370)III;mec-4(e1611)X; hmnIs133],* BP1056 *hyEx68[AFF-*
389 *1::TY1::EGFP::3xFLAG, pRF4, KS]; dzIs53[F49H12.4p::mCherry], AFF-*
390 *1::TY1::EGFP::3xFLAG* was kindly provided by transgenome project (Sarov et al., 2006),
391 BP1055 *hyEx66[AFF-1::TY1::EGFP::3xFLAG, pRF4, KS]; dzIs53,* BP500 *zzIs22*
392 *[pJdC41(eff-1p::EFF-1::GFP), pRF4]; dzIs53 (pF49H12.4::mCherry) zzIs22* was kindly
393 provided by William Mohler (del Campo et al., 2005).

394 **Molecular Biology**

395 The *ser-2prom3::Kaede* (pCY2 plasmid) is a kind gift from Candice Yip and Max Heiman
396 (Yip and Heiman, 2016). It was constructed by digesting *ser-2prom3* with SbfI and AscI and
397 Kaede with AscI and NotI and then ligated together.
398 The *des-2p::AFF-1* construct (pME4 plasmid) was constructed by inserting an AFF-1
399 genomic fragment, digested from *hsp16.2::AFF-1* (Sapir et al., 2007) with NheI and KpnI
400 and cloned into pME2 (Oren-Suissa et al., 2010) cut with the same enzymes. *des-2p::AFF-1*
401 was injected at a concentration of 0.1ng/ml into *eff-1(hy21)* animals and three independent lines
402 were obtained. For dendrotomy experiments, two lines (*hyEx39* and *hyEx391*) were crossed into a
403 wild-type background expressing the PVD marker *ser-2p3::Kaede.*

404 **Live imaging of worms**

405 Time-lapse imaging and short imaging (one time point) of worms by Nomarski optics and
406 fluorescence microscopy was performed using a Nikon eclipse Ti inverted microscope with
407 Yokogawa CSU-X1 spinning disk or using the Zeiss Laser Scanning Microscope (LSM) 510
408 META. Animals were anesthetized using 0.1% tricaine and 0.01% tetramisole in M9

409 solution for 20-30 minutes, and then they were transferred to a 3% agar slide with an eyelash
410 attached to a toothpick. For short time imaging worms were often mounted on 3% agar slides
411 containing 5–10 mM NaN_3 instead. Image acquisition was done using Andor iQ or
412 Metamorph software, when using the spinning disk confocal (SDC), and Zen software when
413 using the LSM 510 meta microscope. Z-stacks were taken with PlanApochromat 60x oil
414 NA=1.4 objective using the SDC or 63x NA=1.4 objective using the LSM. Excitation of
415 GFP and green Kaede was done with 488 nm wavelength laser and 525 filter (6-15%, 50 ms
416 exposure time), RFP and red Kaede was excited with 561 nm wavelength laser and 607 filter
417 (15-20%, 50-100 ms exposure time). When using the sCMOS (Andor) camera z-stacks were
418 taken with ~0.23 µm z-step. With iXon EMCCD camera (Andor) z-stacks were taken with
419 ~0.5 µm z- step, gain was ~100. When the LSM 510 meta was used, z-step was ~0.8 µm.
420 Multidimensional data was reconstructed as maximum intensity projections using the FIJI
421 software (NIH Image). Images were prepared using Imaris, FIJI and Adobe Photoshop CS5.
422 Final figures were constructed using Adobe Illustrator CS5.1.

423 **Laser dendrotomies**

424 Micropoint, pulsed nitrogen laser, or the tunable Chameleon Ultra Ti-Sapphire laser system
425 (two-photon), were used to sever the primary dendrite of the PVD. The Micropoint system
426 was used on the Nikon eclipse Ti inverted microscope with Yokogawa CSU-X1 spinning
427 disk. In order to transect neurons, we used 405 beamsplitter and 365nm dye cell and either
428 IQ or Metamorph software. We used highest levels with the attenuator plate (all the way in),
429 while the software controlled attenuator was adjusted between 80-90% when using IQ, and
430 30-50% when using Metamorph. Roughly 15 pulses at 10 Hz were administered for each cut
431 in IQ and Metamorph. For all worms the primary dendrite was injured anterior to cell body.
432 Animals were imaged and a z-stack was collected immediately after cut to confirm that the
433 injury was successful.

434 The two-photon system was used on the Zeiss LSM 510 META microscope. The
435 laser produces 200fs short pulses at 113MHz repetition rate and energy of 5nJ. In order to
436 cut neurons we used 820 nm wavelength and 20-30% laser power using the Zen software.
437 Worms were imaged immediately after cut to confirm that the injury was successful, and z-
438 stacks were taken using the spinning disk confocal system or the LSM 510 META as
439 described for live imaging of worms. After surgery, animals were recovered on NGM agar
440 plates seeded with OP50 in a drop of M9 and imaged again later, or time-lapse movies were
441 immediately acquired.
442 Regeneration was defined as continuation of the fluorescent signal between the distal and
443 proximal ends or using Kaede photoconversion (**Fig S5**; see below). Significant differences
444 between ages and genotypes were determined using *Fisher's exact test.*

445 **Kaede photoconversion**

446 In order to verify that dendrites fuse as response to injury we used the photoconvertible
447 protein Kaede driven by a PVD specific promoter *ser-2prom3* (Yip and Heiman, 2016).
448 Irreversible photoconversion of the green Kaede to red Kaede was achieved using Mosaic
449 system on the Nikon eclipse Ti inverted microscope with Yokogawa CSU-X1 spinning disk,
450 at 405 nm, 20-50 ms exposure time with 10-20 repeats across the region of interest, which
451 was always the cell body, using either IQ or Metamorph software.

452 **Morphological quantitation of the PVD**

453 Branch count and disorganization of PVD structural units (menorahs) was counted in the 100
454 µm around cell body (unless otherwise stated), as previously described (Oren-Suissa et al.,
455 2010). Lack of self-avoidance between adjacent menorahs was determined in the same
456 region as previously described (Smith et al., 2012). Z-stack maximum intensity projections
457 of time-lapse movies were analyzed manually, using FIJI software. Factorial analysis of
458 variance (ANOVA) and *t-tests* were performed to compare between genotypes and ages.

459 **Harsh touch assay**

460 Harsh touch assay was performed as previously described (Oren-Suissa et al., 2010; Way and
461 Chalfie, 1989) and the experimenter was blind to the genotype. The experiments were done
462 in light touch mutant background (*mec-4(e1611)*) (Chalfie and Sulston, 1981). *mec-3(e1338)*
463 worms were used as negative control (Way and Chalfie, 1989). These mutants are defective
464 in harsh-touch mechanosensation and do not respond to harsh touch. Significant differences
465 between the ages were determined by the $\chi 2$ test.

466 **Life-span assay**

467 Lifespan assays were carried out at 20°C as previously described (Apfeld and Kenyon, 1998).
468 A population of worms was synchronized using hypochlorite and NaOH solution and ~100
469 animals at the L4 "Christmas tree" stage were placed on NGM plates containing 49.5 μM 5-
470 Fluoro-2′-deoxyuridine (FUDR, Sigma, F0503) seeded with OP50 *E. coli*, at a density of 20
471 worms per 6 cm plate. Adult day 1 was designated as the day after the L4 larval stage that
472 served as time 0. Animals were scored as dead or alive every 2-3 days until all animals died.
473 An animal was scored dead when it did not move or react at all to prodding with a platinum
474 wire. Animals that crawled off of the plate, were trapped in fungal infection, "exploded"
475 (i.e., showed extruded tissue from the vulva), or showed internal hatching ("bagging"), were
476 excluded. If plates were contaminated, animals were transferred to fresh plates, using
477 platinum wire. Statistical significance was determined using the Log-Rank (Mantel-Cox)
478 test.

479 **RNA Isolation, Reverse Transcription, and Quantitative Real-Time PCR.**

480 Total RNA from Wild-type worms and des-2p::AFF-1 transgenic worms was isolated using
481 the RNeasy Micro kit following the manufacturer's protocol (Qiagen). RNA was used for
482 cDNA synthesis using the qScript cDNA Synthesis Kit (Quanta BioSciences) with random
483 primers. Real-time PCR was performed using AFF-1 and Fast SYBR® Green Master Mix

484 (Applied Biosystems). The PCR amplification conditions were as follows: 40 cycles of 95 °C
485 for 20 s and 60 °C for 20 s. Each PCR was run in triplicate. Data analysis and quantification
486 were performed using StepOne software V2.2 supplied by Applied Biosystems. To account
487 for the variability in the initial concentration of the RNA, results were normalized to the
488 ACT-1 housekeeping gene.

489 **Statistical analysis**

490 Statistical analysis was performed using the GraphPad online tool:
491 http://www.graphpad.com/quickcalcs/ for *t-tests, Fisher's exact test*s and χ^2 tests. Analysis of
492 variance (ANOVA) that was performed when more than two groups were compared and Log-
493 Rank survival test, using SPSS. *Freeman-Halton* extension of the *Fisher's exact test* (for 2x4
494 contingency table) was performed using the Vassarstats.net online tool, to compare between
495 the distributions of response to injury between different genotypes and ages.

496 **Acknowledgments**

497 We thank D. Cassel, M. Hilliard, and A. Sapir for critically reading earlier versions of the
498 manuscript. M. Heiman and C. Yip for providing CHB392, C. Smith and D. Miller for
499 NC1841, and T. Gattegno for BP709. We also want to thank R. Kishony and all members of
500 the Podbilewicz laboratory for discussion. Some strains were provided by the CGC, which is
501 funded by NIH Office of Research Infrastructure Programs (P40 OD010440).
502 The authors declare no conflict of interest.

503 **Author contributions**

504 VK, MOS and BP designed the experiments. VK performed most experiments. MOS
505 developed the system to study neuronal degeneration and regeneration following dendrotomy
506 using the PVD neurons. MOS generated the PVDp::AFF-1 and PVDp::EFF-1 transgenics and
507 MOS and VK tested the effects of EFF-1 and AFF-1 over-expression on regenerating

animals. BP did some harsh touch assays and supervised this work. VK, MOS and BP wrote the paper.

This article contains supporting information including eight figures and six movies

Funding

This work was supported by the Israel Science Foundation (ISF grant 443/12, to B.P.), the European Research Council (Advanced grant ELEGANSFUSION 268843 to B.P.) and the HFSP long-term postdoctoral fellowship (LT000727/2013L to M.O.S.).

References

Alvarez-Dolado, M., Pardal, R., Garcia-Verdugo, J. M., Fike, J. R., Lee, H. O., Pfeffer, K., Lois, C., Morrison, S. J. and Alvarez-Buylla, A. (2003). Fusion of bone-marrow-derived cells with Purkinje neurons, cardiomyocytes and hepatocytes. *Nature* **425**, 968-973.

Apfeld, J. and Kenyon, C. (1998). Cell nonautonomy of C-elegans daf-2 function in the regulation of diapause and life span. *Cell* **95**, 199-210.

Avinoam, O. and Podbilewicz, B. (2011). Eukaryotic cell-cell fusion families. *Curr Top Membr* **68**, 209-234.

Bekkers, J. M. and Hausser, M. (2007). Targeted dendrotomy reveals active and passive contributions of the dendritic tree to synaptic integration and neuronal output. *Proc Natl Acad Sci U S A* **104**, 11447-11452.

Brenner, S. (1974). Genetics of Caenorhabditis-elegans *Genetics* **77**, 71-94.

Buell, S. J. and Coleman, P. D. (1979). Dendritic growth in the aged human-brain and failure of growth in senile dementia *Science* **206**, 854-856.

Byrne, A. B., Walradt, T., Gardner, K. E., Hubbert, A., Reinke, V. and Hammarlund, M. (2014). Insulin/IGF1 signaling inhibits age-dependent axon regeneration. *Neuron* **81**, 561-573.

Chalfie, M. and Sulston, J. (1981). Developmental genetics of the mechanosensory neurons of Caenorhabditis-elegans *Dev. Biol.* **82**, 358-370.

Chatzigeorgiou, M., Yoo, S., Watson, J. D., Lee, W. H., Spencer, W. C., Kindt, K. S., Hwang, S. W., Miller, D. M., 3rd, Treinin, M., Driscoll, M., et al. (2010). Specific roles for DEG/ENaC and TRP channels in touch and thermosensation in C. elegans nociceptors. *Nature neuroscience* **13**, 861-868.

Chisholm, A. D., Hutter, H., Jin, Y. and Wadsworth, W. G. (2016). The Genetics of Axon Guidance and Axon Regeneration in Caenorhabditis elegans. *Genetics* **204**, 849-882.

Cohen, E., Chatzigeorgiou, M., Husson, S. J., Steuer-Costa, W., Gottschalk, A., Schafer, W. R. and Treinin, M. (2014). Caenorhabditis elegans nicotinic acetylcholine receptors are required for nociception. *Molecular and Cellular Neuroscience* **59**, 85-96.

del Campo, J. J., Opoku-Serebuoh, E., Isaacson, A. B., Scranton, V. L., Tucker, M., Han, M. and Mohler, W. A. (2005). Fusogenic activity of EFF-1 is regulated via dynamic localization in fusing somatic cells of C. elegans. *Curr Biol* **15**, 413-423.

Dong, X., Liu, O. W., Howell, A. S. and Shen, K. (2013). An extracellular adhesion molecule complex patterns dendritic branching and morphogenesis. *Cell* **155**, 296-307.

Dong, X., Shen, K. and Bulow, H. E. (2015). Intrinsic and extrinsic mechanisms of dendritic morphogenesis. *Annu Rev Physiol* **77**, 271-300.

Gabel, C. V., Antonie, F., Chuang, C.-F., Samuel, A. D. T. and Chang, C. (2008). Distinct cellular and molecular mechanisms mediate initial axon development and adult-stage axon regeneration in C. elegans. *Development* **135**, 1129-1136.

Gattegno, T., Mittal, A., Valansi, C., Nguyen, K. C., Hall, D. H., Chernomordik, L. V. and Podbilewicz, B. (2007). Genetic control of fusion pore expansion in the epidermis of Caenorhabditis elegans. *Mol Biol Cell* **18**, 1153-1166.

Ghosh-Roy, A. and Chisholm, A. D. (2010). Caenorhabditis elegans: A new model organism for studies of axon regeneration. *Developmental Dynamics* **239**, 1460-1464.

Ghosh-Roy, A., Wu, Z. L., Goncharov, A., Jin, Y. S. and Chisholm, A. D. (2010). Calcium and cyclic AMP promote axonal regeneration in Caenorhabditis elegans and require DLK-1 kinase. *J. Neurosci.* **30**, 3175-3183.

Giordano-Santini, R., Linton, C. and Hilliard, M. A. (2016). Cell-cell fusion in the nervous system: Alternative mechanisms of development, injury, and repair. *Seminars in cell & developmental biology*.

Hammarlund, M. and Jin, Y. (2014). Axon regeneration in C. elegans. *Current Opinion in Neurobiology* **27**, 199-207.

Hammarlund, M., Nix, P., Hauth, L., Jorgensen, E. M. and Bastiani, M. (2009). Axon regeneration requires a conserved MAP kinase pathway. *Science* **323**, 802-806.

Hoy, R. R., Bittner, G. D. and Kennedy, D. (1967). Regeneration in crustacean motoneurons: evidence for axonal fusion. *Science* **156**, 251-252.

Husson, S. J., Costa, W. S., Wabnig, S., Stirman, J. N., Watson, J. D., Spencer, W. C., Akerboom, J., Looger, L. L., Treinin, M., Miller, D. M., III, et al. (2012). Optogenetic Analysis of a Nociceptor Neuron and Network Reveals Ion Channels Acting Downstream of Primary Sensors. *Current Biology* **22**, 743-752.

Jan, Y. N. and Jan, L. Y. (2010). Branching out: mechanisms of dendritic arborization. *Nat. Rev. Neurosci.* **11**, 316-328.

Johansson, C. B., Youssef, S., Koleckar, K., Holbrook, C., Doyonnas, R., Corbel, S. Y., Steinman, L., Rossi, F. M. V. and Blau, H. M. (2008). Extensive fusion of haematopoietic cells with Purkinje neurons in response to chronic inflammation. *Nature Cell Biology* **10**, 575-583.

575 **Kenyon, C., Chang, J., Gensch, E., Rudner, A. and Tabtiang, R.** (1993). A C-elegans mutant the lives twice
576 as long as wild- type *Nature* **366**, 461-464.
577 **Kenyon, C. J.** (2010). The genetics of ageing. *Nature* **464**, 504-512.
578 **Koleske, A. J.** (2013). Molecular mechanisms of dendrite stability. *Nat. Rev. Neurosci.* **14**, 536-550.
579 **Lenard, A., Daetwyler, S., Betz, C., Ellertsdottir, E., Belting, H.-G., Huisken, J. and Affolter, M.** (2015).
580 Endothelial cell self-fusion during vascular pruning. *PLoS biology* **13**, e1002126-e1002126.
581 **Lin, K., Hsin, H., Libina, N. and Kenyon, C.** (2001). Regulation of the Caenorhabditis elegans longevity
582 protein DAF-16 by insulin/IGF-1 and germline signaling. *Nature Genetics* **28**, 139-145.
583 **Liu, O. W. and Shen, K.** (2011). The transmembrane LRR protein DMA-1 promotes dendrite branching and
584 growth in C. elegans. *Nat Neurosci* **15**, 57-63.
585 **Maletic-Savatic, M., Malinow, R. and Svoboda, K.** (1999). Rapid dendritic morphogenesis in CA1
586 hippocampal dendrites induced by synaptic activity. *Science* **283**, 1923-1927.
587 **Maniar, T. A., Kaplan, M., Wang, G. J., Shen, K., Wei, L., Shaw, J. E., Koushika, S. P. and Bargmann, C.**
588 **I.** (2012). UNC-33 (CRMP) and ankyrin organize microtubules and localize kinesin to polarize axon-
589 dendrite sorting. *Nat Neurosci* **15**, 48-56.
590 **Mohler, W. A., Shemer, G., del Campo, J., Valansi, C., Opoku-Serebuoh, E., Scranton, V., Assaf, N.,**
591 **White, J. G. and Podbilewicz, B.** (2002). The type I membrane protein EFF-1 is essential for
592 developmental cell fusion in *C. elegans*. *Dev Cell* **2**, 355-362.
593 **Murphy, C. T., McCarroll, S. A., Bargmann, C. I., Fraser, A., Kamath, R. S., Ahringer, J., Li, H. and**
594 **Kenyon, C.** (2003). Genes that act downstream of DAF-16 to influence the lifespan of Caenorhabditis
595 elegans. *Nature* **424**, 277-284.
596 **Nawabi, H., Zukor, K. and He, Z.** (2012). No simpler than mammals: axon and dendrite regeneration in
597 Drosophila. *Genes Dev* **26**, 1509-1514.
598 **Neumann, B., Coakley, S., Giordano-Santini, R., Linton, C., Lee, E. S., Nakagawa, A., Xue, D. and**
599 **Hilliard, M. A.** (2015). EFF-1-mediated regenerative axonal fusion requires components of the
600 apoptotic pathway. *Nature* **517**, 219-222.
601 **Neumann, B., Nguyen, K. C. Q., Hall, D. H., Ben-Yakar, A. and Hilliard, M. A.** (2011). Axonal
602 Regeneration Proceeds Through Specific Axonal Fusion in Transected C. elegans Neurons.
603 *Developmental Dynamics* **240**, 1365-1372.
604 **Oren-Suissa, M., Gattegno, T., Kravtsov, V. and Podbilewicz, B.** (2017). Extrinsic Repair of Injured
605 Dendrites as a Paradigm for Regeneration by Fusion in Caenorhabditis elegans. *Genetics*.
606 https://doi.org/10.1534/genetics.116.196386
607 **Oren-Suissa, M., Hall, D., Treinin, M., Shemer, G. and Podbilewicz, B.** (2010). The Fusogen EFF-1
608 Controls Sculpting of Mechanosensory Dendrites. *Science* **328**, 1285-1288.
609 **Paltsyn, A., Komissarova, S., Dubrovin, I. and Kubatiev, A.** (2013). Increased cell fusion in cerebral cortex
610 may contribute to poststroke regeneration. *Stroke research and treatment* **2013**, 869327-869327.
611 **Pan, C.-L., Peng, C.-Y., Chen, C.-H. and McIntire, S.** (2011). Genetic analysis of age-dependent defects of
612 the Caenorhabditis elegans touch receptor neurons. *Proc. Natl. Acad. Sci. U.S.A.* **108**, 9274-9279.
613 **Park, K. K., Liu, K., Hu, Y., Smith, P. D., Wang, C., Cai, B., Xu, B., Connolly, L., Kramvis, I., Sahin, M.,**
614 **et al.** (2008). Promoting axon regeneration in the adult CNS by modulation of the PTEN/mTOR
615 pathway. *Science* **322**, 963-966.
616 **Pérez-Vargas, J., Krey, T., Valansi, C., Avinoam, O., Haouz, A., Jamin, M., Raveh-Barak, H.,**
617 **Podbilewicz, B. and Rey, F. A.** (2014). Structural basis of eukaryotic cell-cell fusion. *Cell* **157**, 407-
618 419.
619 **Pestronk, A., Drachman, D. B. and Griffin, J. W.** (1980). Effects of aging on nerve sprouting and
620 regeneration *Exp. Neurol.* **70**, 65-82.
621 **Podbilewicz, B., Leikina, E., Sapir, A., Valansi, C., Suissa, M., Shemer, G. and Chernomordik, L. V.**
622 (2006). The C. elegans developmental fusogen EFF-1 mediates homotypic fusion in heterologous cells
623 and in vivo. *Dev Cell* **11**, 471-481.
624 **Procko, C., Lu, Y. and Shaham, S.** (2011). Glia delimit shape changes of sensory neuron receptive endings in
625 C. elegans. *Development* **138**, 1371-1381.
626 **Rao, K., Stone, M. C., Weiner, A. T., Gheres, K. W., Zhou, C., Deitcher, D. L., Levitan, E. S. and Rolls,**
627 **M. M.** (2016). Spastin, atlastin, and ER relocalization are involved in axon but not dendrite
628 regeneration. *Mol Biol Cell* **27**, 3245-3256.
629 **Rasmussen, J. P., English, K., Tenlen, J. R. and Priess, J. R.** (2008). Notch signaling and morphogenesis of
630 single-cell tubes in the C. elegans digestive tract. *Dev Cell* **14**, 559-569.
631 **Ruschel, J., Hellal, F., Flynn, K. C., Dupraz, S., Elliott, D. A., Tedeschi, A., Bates, M., Sliwinski, C.,**
632 **Brook, G., Dobrindt, K., et al.** (2015). Axonal regeneration. Systemic administration of epothilone B
633 promotes axon regeneration after spinal cord injury. *Science* **348**, 347-352.

Salzberg, Y., Diaz-Balzac, C. A., Ramirez-Suarez, N. J., Attreed, M., Tecle, E., Desbois, M., Kaprielian, Z. and Buelow, H. E. (2013). Skin-derived cues control arborization of sensory dendrites in Caenorhabditis elegans. *Cell* **155**, 308-320.

Sapir, A., Choi, J., Leikina, E., Avinoam, O., Valansi, C., Chernomordik, L. V., Newman, A. P. and Podbilewicz, B. (2007). AFF-1, a FOS-1-regulated fusogen, mediates fusion of the anchor cell in C-elegans. *Dev. Cell* **12**, 683-698.

Sarov, M., Schneider, S., Pozniakovski, A., Roguev, A., Ernst, S., Zhang, Y., Hyman, A. A. and Stewart, A. F. (2006). A recombineering pipeline for functional genomics applied to Caenorhabditis elegans. *Nat Methods* **3**, 839-844.

Shemer, G., Suissa, M., Kolotuev, I., Nguyen, K. C. Q., Hall, D. H. and Podbilewicz, B. (2004). EFF-1 is sufficient to initiate and execute tissue-specific cell fusion in *C. elegans*. *Curr Biol* **14**, 1587-1591.

Smith, C. J., Watson, J. D., Spencer, W. C., O'Brien, T., Cha, B., Albeg, A., Treinin, M. and Miller, D. M., 3rd (2010). Time-lapse imaging and cell-specific expression profiling reveal dynamic branching and molecular determinants of a multi-dendritic nociceptor in C. elegans. *Dev Biol* **345**, 18-33.

Smith, C. J., Watson, J. D., VanHoven, M. K., Colon-Ramos, D. A. and Miller, D. M., 3rd (2012). Netrin (UNC-6) mediates dendritic self-avoidance. *Nat Neurosci* **15**, 731-737.

Smurova, K. and Podbilewicz, B. (2016). RAB-5- and DYNAMIN-1-Mediated Endocytosis of EFF-1 Fusogen Controls Cell-Cell Fusion. *Cell reports* **14**, 1517-1527.

Soulavie, F. and Sundaram, M. V. (2016). Auto-fusion and the shaping of neurons and tubes. *Seminars in cell & developmental biology* **60**, 136-145.

Stone, C. E., Hall, D. H. and Sundaram, M. V. (2009). Lipocalin signaling controls unicellular tube development in the Caenorhabditis elegans excretory system. *Dev Biol* **329**, 201-211.

Tank, E. M. H., Rodgers, K. E. and Kenyon, C. (2011). Spontaneous age-related neurite branching in Caenorhabditis elegans. *J. Neurosci.* **31**, 9279-9288.

Taylor, A. M., Blurton-Jones, M., Rhee, S. W., Cribbs, D. H., Cotman, C. W. and Jeon, N. L. (2005). A microfluidic culture platform for CNS axonal injury, regeneration and transport. *Nat Methods* **2**, 599-605.

Thompson-Peer, K. L., DeVault, L., Li, T., Jan, L. Y. and Jan, Y. N. (2016). In vivo dendrite regeneration after injury is different from dendrite development. *Genes Dev* **30**, 1776-1789.

Toth, M. L., Melentijevic, I., Shah, L., Bhatia, A., Lu, K., Talwar, A., Naji, H., Ibanez-Ventoso, C., Ghose, P., Jevince, A., et al. (2012). Neurite sprouting and synapse deterioration in the aging Caenorhabditis elegans nervous system. *J. Neurosci.* **32**, 8778-8790.

Tsalik, E. L., Niacaris, T., Wenick, A. S., Pau, K., Avery, L. and Hobert, O. (2003). LIM homeobox gene-dependent expression of biogenic amine receptors in restricted regions of the C-elegans nervous system. *Developmental Biology* **263**, 81-102.

Verdu, E., Ceballos, D., Vilches, J. J. and Navarro, X. (2000). Influence of aging on peripheral nerve function and regeneration. *J. Periph. Nerv. Syst.* **5**, 191-208.

Way, J. C. and Chalfie, M. (1989). The mec-3 gene of Caenorhabditis-elegans requires its own product for maintained expression and is expressed in 3 neuronal cell-types *Genes Dev.* **3**, 1823-1833.

Wei, X., Howell, A. S., Dong, X., Taylor, C. A., Cooper, R. C., Zhang, J., Zou, W., Sherwood, D. R. and Shen, K. (2015). The unfolded protein response is required for dendrite morphogenesis. *eLife* **4**, e06963.

Yang, Y., Zhang, Y., Li, W. J., Jiang, Y., Zhu, Z., Hu, H., Li, W., Wu, J. W., Wang, Z. X., Dong, M. Q., et al. (2017). Spectraplakin Induces Positive Feedback between Fusogens and the Actin Cytoskeleton to Promote Cell-Cell Fusion. *Dev Cell* **41**, 107-120 e104.

Yaniv, S. P., Issman-Zecharya, N., Oren-Suissa, M., Podbilewicz, B. and Schuldiner, O. (2012). Axon Regrowth during Development and Regeneration Following Injury Share Molecular Mechanisms. *Curr Biol* **22**, 1774-1782.

Yankner, B. A., Lu, T. and Loerch, P. (2008). The aging brain. *Annu Rev Pathol* **3**, 41-66.

Yip, Z. C. and Heiman, M. G. (2016). Duplication of a Single Neuron in C. elegans Reveals a Pathway for Dendrite Tiling by Mutual Repulsion. *Cell reports* **15**, 2109-2117.

Zou, Y., Chiu, H., Zinovyeva, A., Ambros, V., Chuang, C.-F. and Chang, C. (2013). Developmental decline in neuronal regeneration by the progressive change of two intrinsic timers. *Science* **340**, 372-376.

690 **Figure legends**
691
692 **Fig 1. PVD's dendritic alterations during aging**

693 **(A-D)** PVD in wild-type (wt; **A** and **C**) and *daf-2* mutants (**B** and **D**) at L4 stage and 9 days
694 of adulthood (9d). Upper panels, magnified boxed areas with candelabra-shaped units colored
695 according to the scheme (**A).** c, cell body. Scale bars, 50 µm and 20 µm in magnified images.
696 Anterior is left and ventral is down in all the figures. Filled arrows, self-avoidance defects.
697 Empty arrows, disorganized menorahs.

698 **(E-I)** Quantitation of phenotypes. Percentages were calculated for 100 µm of length around
699 the cell body. Error bars, ± s.e.m. (**E**) There is no significant difference between wild-type
700 animals and *daf-2* mutant animals at any age (one-way ANOVA). However, there is a
701 significant difference between different developmental stages of the same genotype.(**F-G**)
702 According to ANOVA age gives a significant difference in 4ry and in 5-7ry branching
703 number both in wt and in *daf-2* backgrounds. (**H-I**) According to one-way ANOVA age has
704 significance in menorahs disorganization and loss of self- avoidance in both wild-type and
705 *daf-2.* Statistics were calculated using one way ANOVA followed by post-hoc analysis of
706 student's t-test with Benferroni correction. * *P<0.05,* ** *P<0.01,* *** *P<0.001,* ****
707 *P<0.0001.* Number of animals analyzed: wt L4, *daf-2* L4 and *daf-2* 5d n=10, wt 5d n=9, wt
708 9d n=6, *daf-2* 9d n=8.
709

710 **Fig 2. DAF-2-DAF-16 control self-avoidance at L4 stage**

711 **(A)** Image showing four wild-type PVD dendritic units labeled with GFP, two of them do not
712 overlap (filled arrow) and two show defective self-avoidance (empty arrow).

713 **(B)** Percentage of defects in self-avoidance in 100 µm of length around PVD cell body at L4
714 stage in different genotypes, n ≥ 7. Defective self-avoidance increases in *daf-2* mutants in a
715 *daf-16*-dependent manner. Error bars are ± s.e.m. Statistics were calculated using one way
716 ANOVA followed by post-hoc analysis of student's t-test with Benferroni correction. *
717 P<0.05. Number of animals analyzed: wt n=7, *daf-2* n=12, *daf-16* n=11, *daf-2;daf-16* n=7
718
719 **Fig 3. Adults show a reduction in dendritic plasticity**

720 **(A)** Time-lapse confocal projections of 5 days of adulthood (5d) wild-type animal. Boxed
721 areas are enlarged in the lower panel and reveal dynamic growth (arrows) and retraction
722 (arrowheads) of branches. Scale bars, 10 µm.

723 **(B)** Growth and retraction rates in µm/minute of branches at L4 stage and 5d as measured
724 from time-lapse movies. ≥ 18 branches were analyzed from 4 L4 animals and 2 5d animals.
725 Error bars are ± s.e.m. *P* values from *t* tests: ** *P<0.01,* *** *P<0.001*. See also **Movie S1**.

726

727 **Fig 4. Decline in response to harsh touch during aging in both wild-type and *daf-2***

728 **(A-D)** PVD's cell-body region of wt and light-touch insensitive *mec-4* mutants at the L4
729 stage and at 5 days of adulthood (5d). Scale bars are 20 µm.

730 **(E)** Total number of branches counted in 100 µm of length around cell-body in wt and *mec-4*
731 mutants at L4 and 5d (no significant differences between wt and *mec-4)*. Error bars are ±
732 s.e.m. Number of animals analyzed: wt L4 and *mec-4* 5d n=7, wt 5d and *mec-4* L4 n=5
733
734 **(F)** Percentage of animals responding to harsh touch by escaping away from the stimulus. At
735 the age of 5d, the response declined in *mec-4* light-touch defective mutants and in *daf-2;mec-*
736 *4* double mutants. *mec-3* mutants are defective in harsh-touch mechanosensation and do not
737 respond to harsh touch. We performed a one way ANOVA statistical test and found no
738 significant difference between wt and *mec-4* animals (at any age), or between any of the
739 backgrounds (chi square test). Number of animals analyzed: 1d *mec-3* n=88, *mec-4* n=70,
740 *daf-2;mec-4* n=45, wt n=39; d3 *mec-3* n=57, *mec-4* n=70, *daf-2;mec-4* n=55, wt n=26; d5
741 *mec-3* n=68, *mec-4* n=134, *daf-2;mec-4* n=41, wt n=95.

742

743 **Fig 5. EFF-1 overexpression in the PVD simplifies aged dendritic trees**

744 **(A-D)** Inverted fluorescence images of PVD neurons.
745 (**A** and **C)** Represent wild-type neurons from L4 and 9 days of adulthood (9d).
746 (**B** and **D)** Represent EFF-1 overexpression under PVD specific promoter (PVDp) at L4 and
747 9d. In each panel one candelabrum unit (boxed) is enlarged and colored (see **Figure 1A**).
748 Scale bars, 20 µm and 10 µm in the enlarged images.
749 **(E-G)** Graphs showing number of branches in 100 µm of length around cell body. Error bars,
750 ± s.e.m. According to one way ANOVA test, age is a significant factor when comparing
751 number of branches (*p<0.0001*). *p* values from *t* tests: * *p<0.05, *** p<0.001, ****
752 *p<0.0001* Number of animals analyzed: wt L4 n=8, wt 9-10d n=5, PVDp::EFF-1 line 1 L4
753 n=12 and 9-10d n=4, PVDp::EFF-1 line 2 L4 n=15 and 9-10d n=21. PVDp::EFF-1 line 1 and
754 2 correspond to worms carrying the extrachromosomal arrays *hyEx392* and *hyEx23,*
755 respectively.

756

757 **Fig 6. *daf-2*(-) restores regenerative ability of aged animals via *daf-16***

758 **(A-D)** PVD neurons immediately after cut and 24 h later in wild-type and *daf-2* mutants at L4
759 and 5 days of adulthood (5d), as indicated. Schematic illustrations below negative images.
760 Red lightings, injury sites. Blue arrows, fusion sites (successful regeneration). Scale bars, 20
761 µm.

762 **(E)** Response to injury of wild-types at L4-young adult (YA) and 2-3d within a short time (3-
763 6 h) after injury. Number of animals: n=7 (L4 –YA) and n=4 (2-3d).

764 **(F)** Percentage of successfully regenerating animals within 24-48 h post injury. Statistics
765 were calculated using *Fisher's exact tests * p<0.05*, *** p<0.01, *** p<0.001.* Number of
766 animals analyzed: wt L4 n=22, wt 5D n=16, *daf-2* L4 n=24, *daf-2* 5d n=12, *daf-16* L4 n=13,
767 *daf-16* 5d n=10. See also **Movies S2-S4**.

768

769

770 **Fig 7. AFF-1 enhances regeneration by dendrite fusion in 5d-old animals**

771 **(A-B)** Inverted fluorescence images of PVD neurons immediately after cut and 24 hours (h)
772 later in animals overexpressing AFF-1 in the PVD (PVDp::AFF-1), at L4 and 5 days of
773 adulthood (5d), as indicated on each image (schematic drawings below each image). Red
774 lightning marks the injury site and blue arrows point at dendrite fusion sites**.** Scale bars, 20
775 μm.

776 **(C)** Percentage of successfully regenerating animals within 24-48h after injury. *p* value from
777 *Fisher's exact test*: * *P<0.05;* *** *P<0.001*. Number of animals analyzed: wt L4 n=22, wt 5d
778 n=16, PVDp::AFF-1 line 1 L4 n=17, 5d n=10, PVDp::AFF-1 line 2 L4 n=15, 5d n=11. See
779 also **Movies S5-S6**. PVDp::AFF-1 line 1 and 2 correspond to worms carrying the
780 extrachromosomal arrays *hyEx39* and *hyEx391,* respectively.

781

782 **Fig 8. *daf-2*(-) and AFF-1(+) rejuvenate fusion potential of broken dendrites**

783 **(A)** Cartoon representing four possible outcomes of dendrotomy. Dendrite auto-fusion
784 indicates successful regeneration (outcomes 1-3), if fusion does not occur degeneration takes
785 place (outcome 4).

786 **(B-J)** Percentages of wild-type worms (wt), *daf-2* mutants and AFF-1 overexpressing animals
787 (PVDp::AFF-1) at different ages, divided into the four different types of response to injury as
788 described in (**A**). Genotype and age are listed above each plot. *p* values from *Fisher's exact*
789 *tests*: * *p<0.05*, ** *p<0.01,* *** *p<0.001.* Additional significant differences were found
790 between: (**C** and **F**), (**C** and **I**) and between (**B** and **J**) (*p<0.05*).
791

792 **Fig 9. Model of morphological and regenerative antiaging activities on dendritic arbors**

793 ***Morphological aging*** of PVD menorahs is a progressive and dynamic process that results in
794 loss of self-avoidance, disorganization and hyperbranching. When the fusogen EFF-1 is
795 ectopically expressed in the PVD neuron it has an antiaging activity that involves pruning of
796 hyperbranched dendritic trees.

797 **Aged menorahs lose their *regenerative potential*** because following laser-induced
798 dendrotomy old neurons usually fail to auto-fuse broken dendrites and undergo degeneration.
799 DAF-2/ IGF-1R negatively regulates the regeneration process. When the fusogen AFF-1 is
800 ectopically expressed in the PVD neuron it has an antiaging activity that promotes auto-
801 fusion of old transected primary dendrites.
802

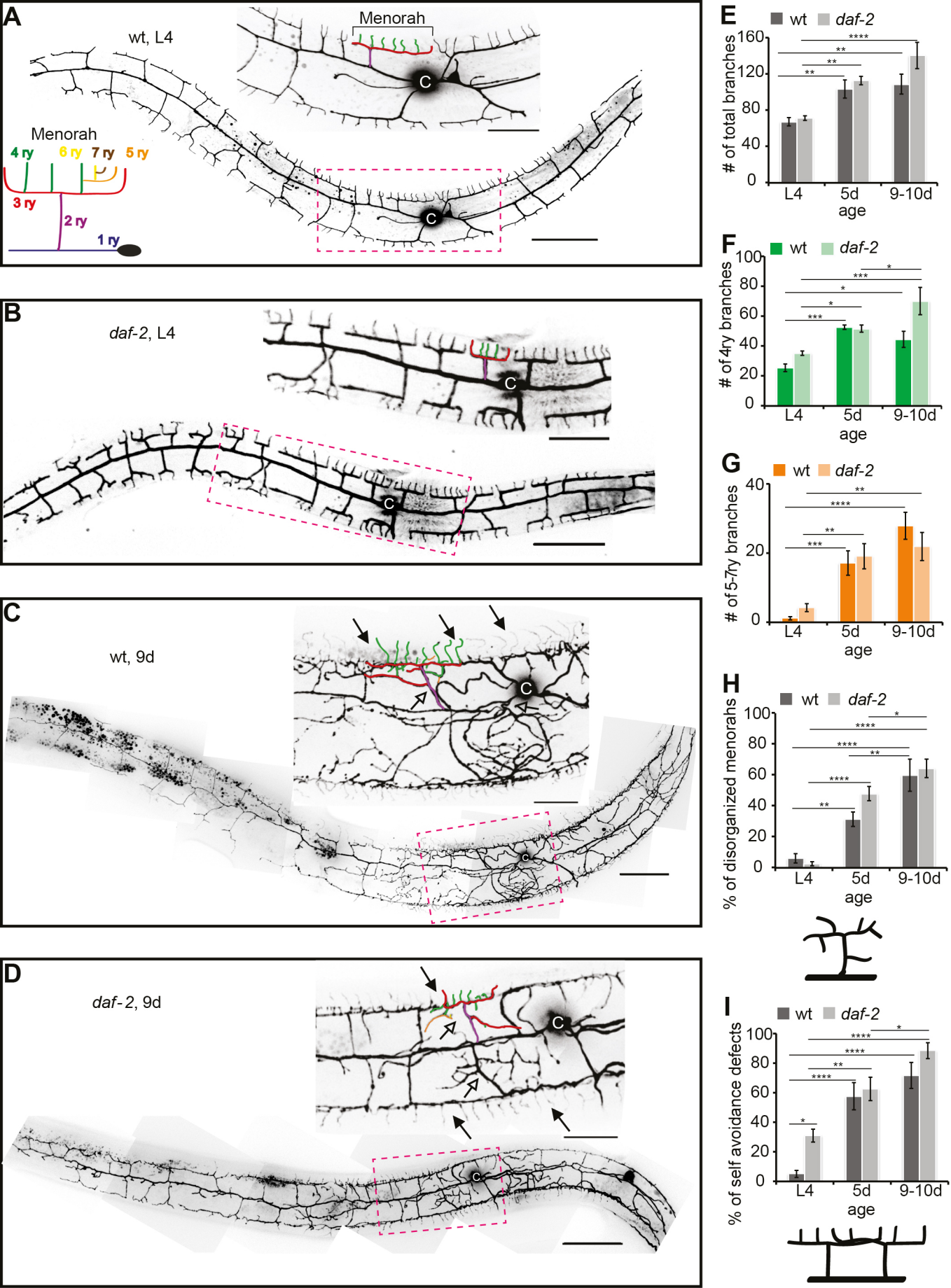
A
wt, L4
Menorah
C
Menorah
4 ry
6 ry
7 ry
5 ry
3 ry
2 ry
1 ry
B
daf-2, L4
C
C
C
wt, 9d
C
C
D
daf-2, 9d
C
C
E
wt
daf-2
# of total branches
age
L4
5d
9-10d
F
# of 4ry branches
G
# of 5-7ry branches
H
% of disorganized menorahs
I
% of self avoidance defects

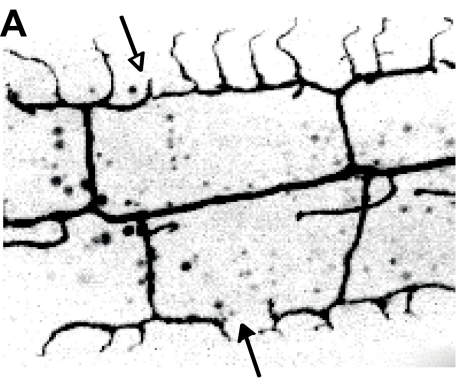
A

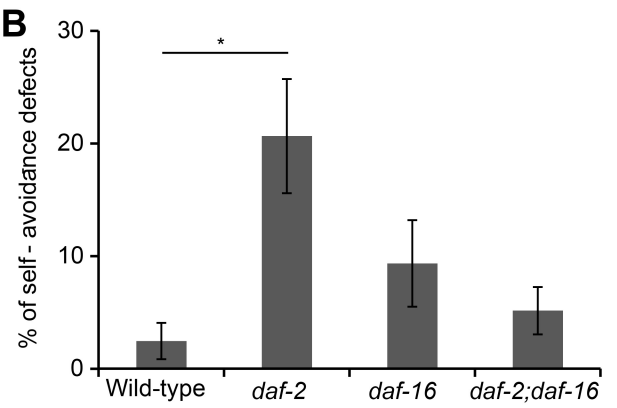
B
% of self - avoidance defects
30
20
10
0
*
Wild-type
daf-2
daf-16
daf-2;daf-16

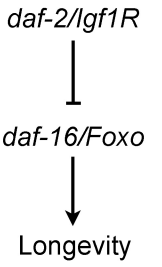
daf-2/Igf1R
daf-16/Foxo
Longevity

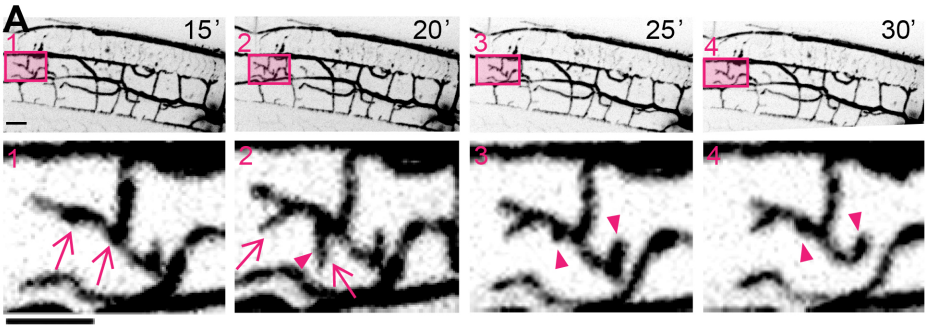
A
15'
20'
25'
30'
1
2
3
4

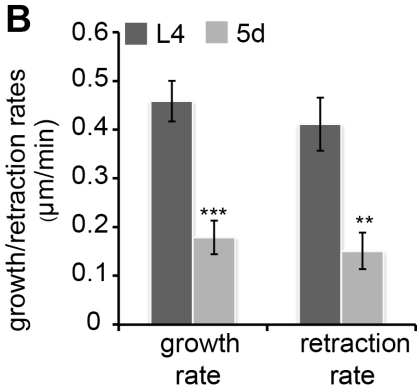
B
L4
5d
growth/retraction rates (µm/min)
0.6
0.5
0.4
0.3
0.2
0.1
0
***
**
growth rate
retraction rate

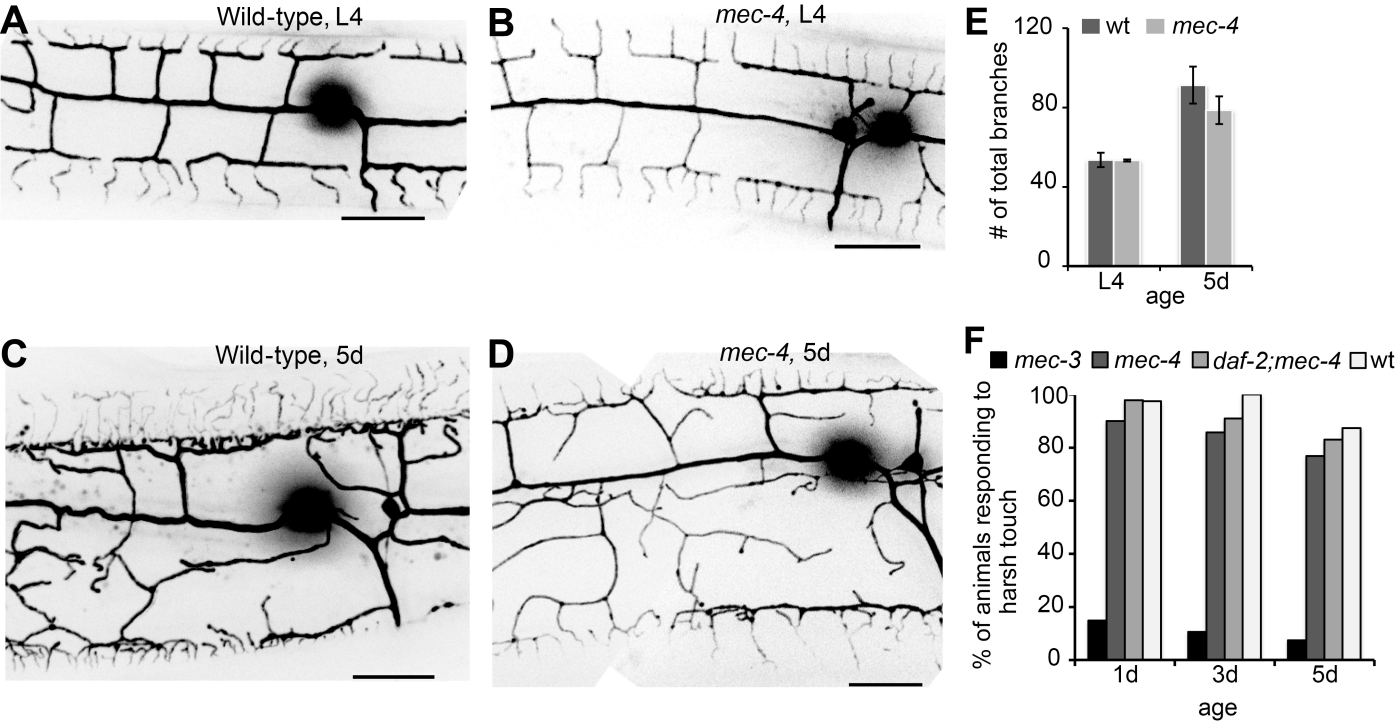
A
Wild-type, L4
B
mec-4, L4
C
Wild-type, 5d
D
mec-4, 5d
E
wt
mec-4
# of total branches
120
80
40
0
L4
5d
age
F
mec-3
mec-4
daf-2;mec-4
wt
% of animals responding to harsh touch
100
80
60
40
20
0
1d
3d
5d
age

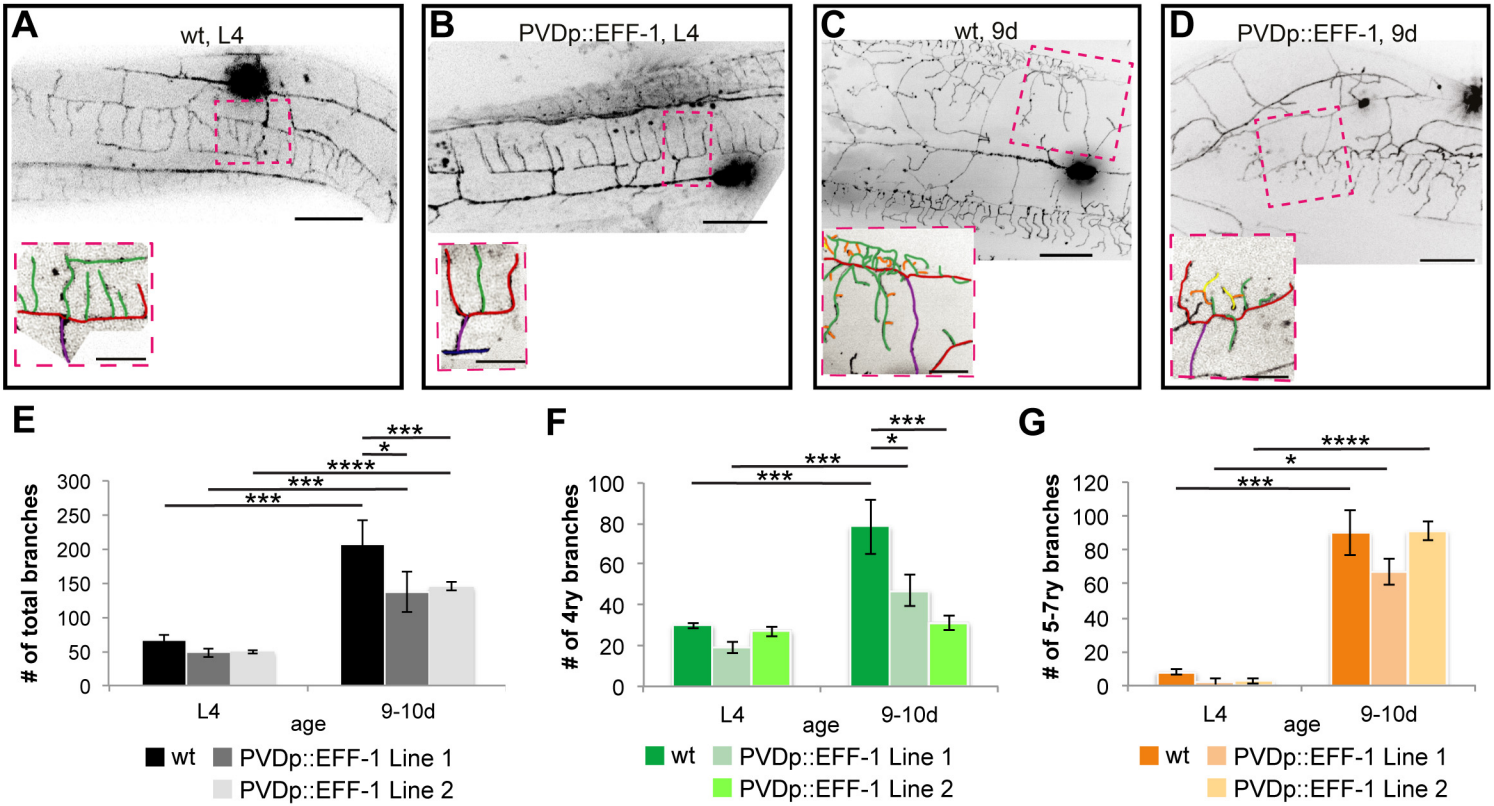
A
wt, L4
B
PVDp::EFF-1, L4
C
wt, 9d
D
PVDp::EFF-1, 9d
E
# of total branches
300
250
200
150
100
50
0
***
***
****
*
***
L4
9-10d
age
wt
PVDp::EFF-1 Line 1
PVDp::EFF-1 Line 2
F
# of 4ry branches
100
80
60
40
20
0
***
***
*
***
L4
9-10d
age
wt
PVDp::EFF-1 Line 1
PVDp::EFF-1 Line 2
G
# of 5-7ry branches
120
100
80
60
40
20
0
***
*
****
L4
9-10d
age
wt
PVDp::EFF-1 Line 1
PVDp::EFF-1 Line 2

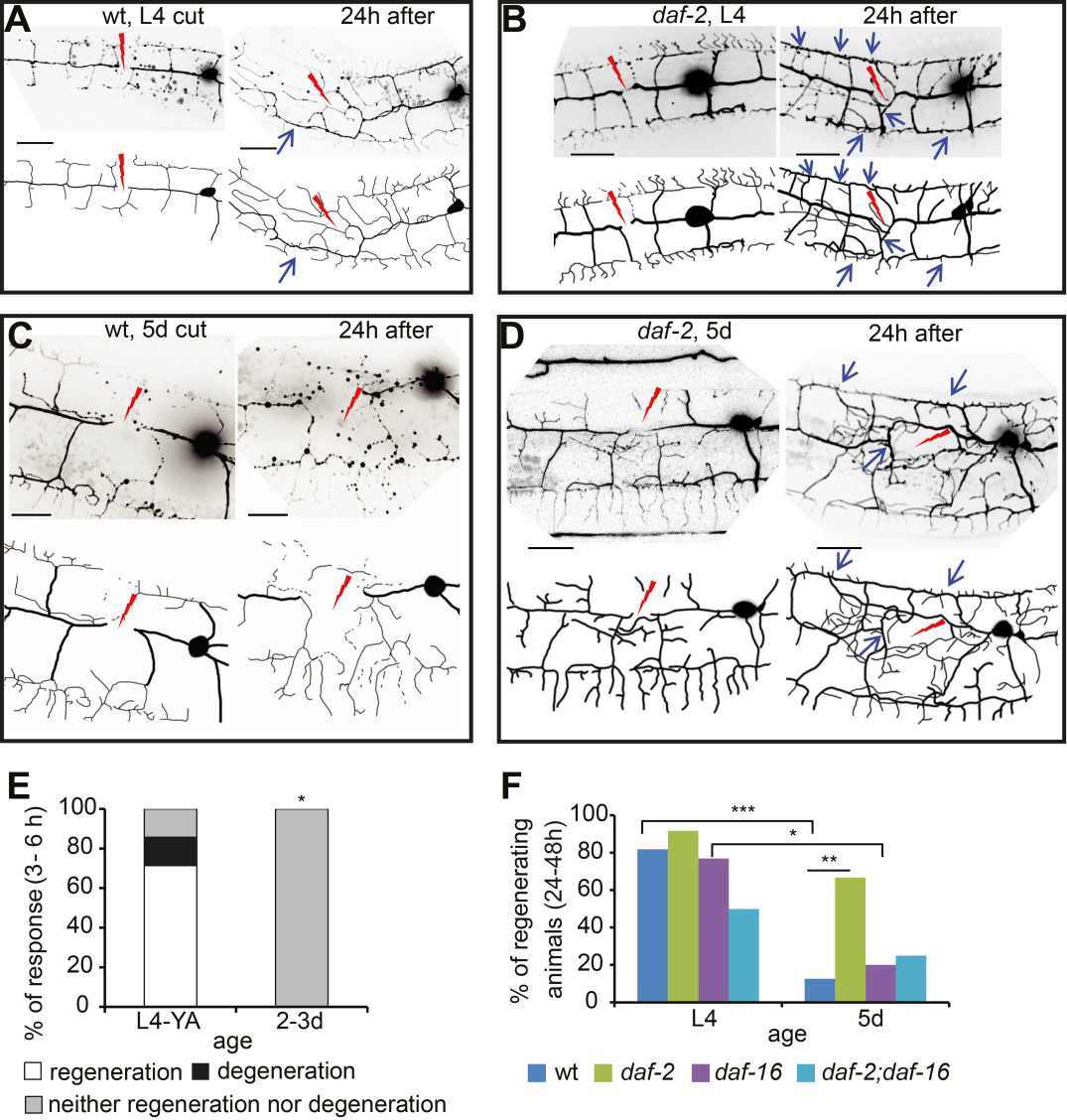
A
wt, L4 cut
24h after
B
daf-2, L4
24h after
C
wt, 5d cut
24h after
D
daf-2, 5d
24h after
E
% of response (3- 6 h)
100
80
60
40
20
0
*
L4-YA
2-3d
age
regeneration
degeneration
neither regeneration nor degeneration
F
% of regenerating animals (24-48h)
100
80
60
40
20
0
***
*
**
L4
5d
age
wt
daf-2
daf-16
daf-2;daf-16

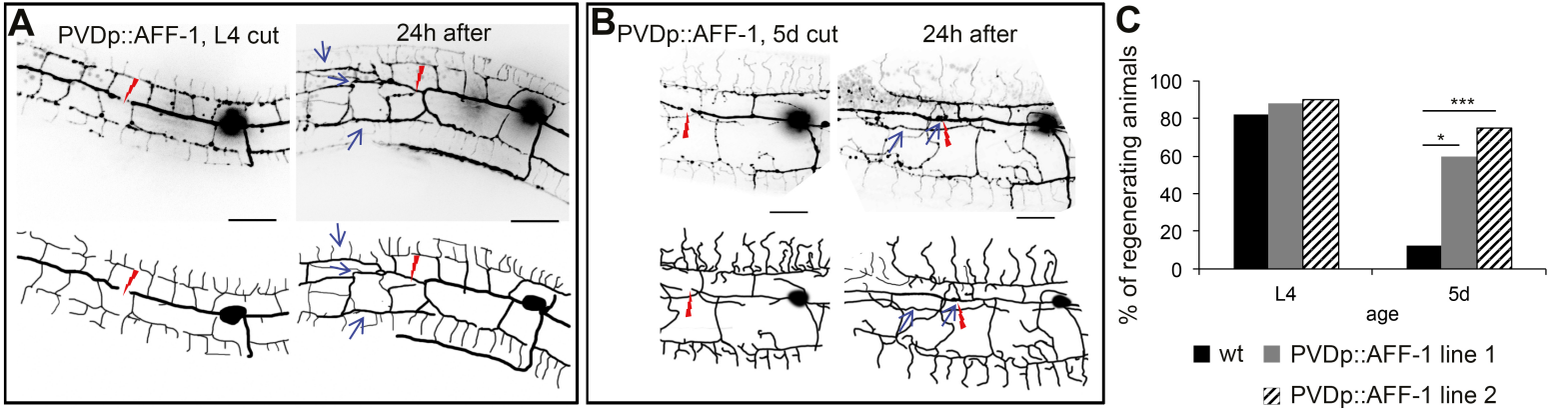
A
PVDp::AFF-1, L4 cut
24h after
B
PVDp::AFF-1, 5d cut
24h after
C
% of regenerating animals
100
80
60
40
20
0
***
*
L4
5d
age
wt
PVDp::AFF-1 line 1
PVDp::AFF-1 line 2

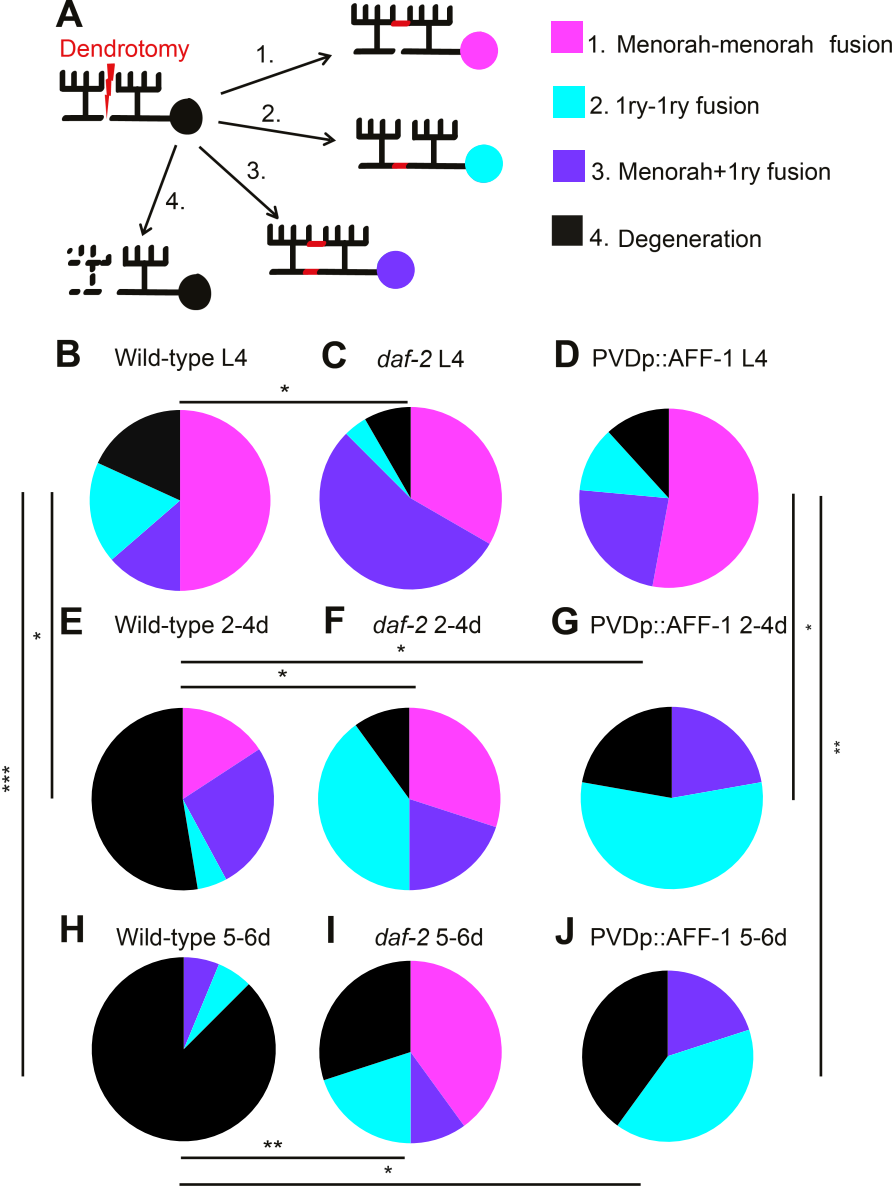
A
Dendrotomy
1.
2.
3.
4.
1. Menorah-menorah fusion
2. 1ry-1ry fusion
3. Menorah+1ry fusion
4. Degeneration
B Wild-type L4
C daf-2 L4
D PVDp::AFF-1 L4
E Wild-type 2-4d
F daf-2 2-4d
G PVDp::AFF-1 2-4d
H Wild-type 5-6d
I daf-2 5-6d
J PVDp::AFF-1 5-6d
*
*
*
*
*
**
***
**
*

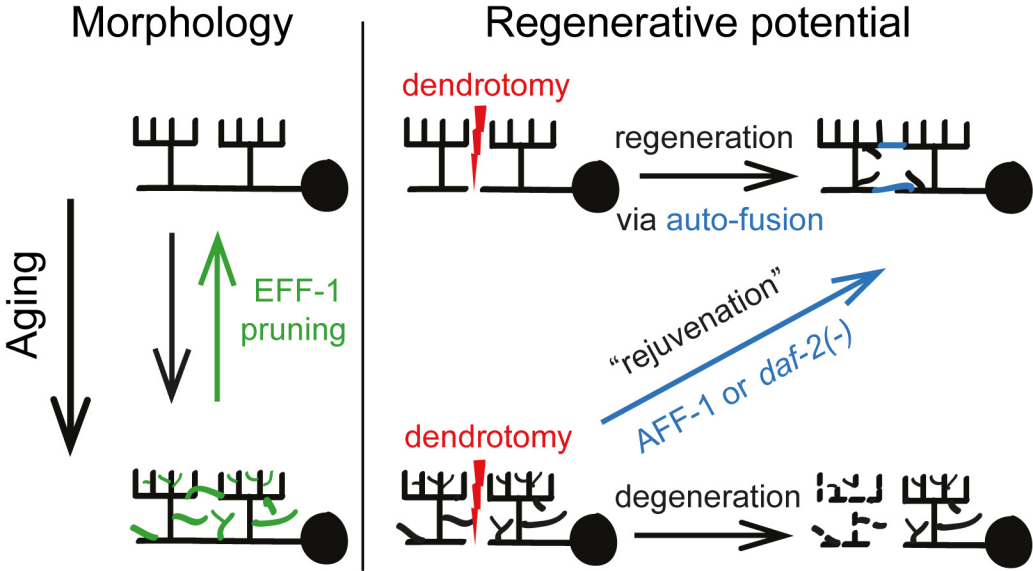
Morphology
Regenerative potential
Aging
EFF-1
pruning
dendrotomy
regeneration
via auto-fusion
"rejuvenation"
AFF-1 or daf-2(-)
dendrotomy
degeneration